

Hydrogen bonding characterization in water and small molecules

Pier Luigi Silvestrelli

*Dipartimento di Fisica e Astronomia, Università di Padova,
via Marzolo 8, I-35131, Padova, Italy*

Abstract

The prototypical Hydrogen bond in water dimer and Hydrogen bonds in the protonated water dimer, in other small molecules, in water cyclic clusters, and in ice, covering a wide range of bond strengths, are theoretically investigated by first-principles calculations based on the Density Functional Theory, considering a standard Generalized Gradient Approximation functional but also, for the water dimer, hybrid and van-der-Waals corrected functionals. We compute structural, energetic, and electrostatic (induced molecular dipole moments) properties. In particular, Hydrogen bonds are characterized in terms of differential electron densities distributions and profiles, and of the shifts of the centres of Maximally localized Wannier Functions. The information from the latter quantities can be conveyed into a single geometric bonding parameter that appears to be correlated to the Mayer bond order parameter and can be taken as an estimate of the covalent contribution to the Hydrogen bond. By considering the cyclic water hexamer and the hexagonal phase of ice we also elucidate the importance of cooperative/anticooperative effects in Hydrogen-bonding formation.

I. INTRODUCTION

The Hydrogen bond (HB), namely the pairwise interaction between an electronegative atom and a H covalently bound to another electronegative atom, is a relatively weak (often of the order of 100-300 meV/HB^{1,2}) bond of paramount importance, being the most effective of all directional intermolecular interactions. For instance, it is the interaction which determines the peculiar properties of water in the condensed phases, and holds together the two strands of DNA in the double helix and the 3-dimensional structure of proteins.¹ Moreover, HBs play a vital role in the chemistry of life because they can easily be made and broken at ambient temperatures.³ Actually there are several different types of HBs and dissociation energies span more than 2 orders of magnitude, from 0.2 to 40 kcal/mol (from 0.01 to 1.7 eV); this wide range means that different types of interaction energies, i.e. electrostatic, induction, electron delocalization, exchange repulsion and dispersion give different relative contributions to the overall energy of the HB; however, for the vast majority of normal HB in the vapor and condensed phases, the electrostatic-plus-induction description seems to provide a near quantitative account of the attractive force responsible for the interaction.^{3,4}

The directional interaction between water molecules is the *prototype* of all HBs and can be termed the “classical HB” (of moderate strength):⁴ the O-H bonds of a water molecule are inherently polar with partial atomic charges of around $+0.4e$ on each H atom and $-0.8e$ on O. In water the intermolecular distance is shortened by around 1 Å compared to the sum of the van der Waals (vdW) radii for the H and O atoms, which indicates a substantial overlap of electron orbitals to form a 3-center, 4-electron bond; despite significant charge transfer in the HB of the water dimer, the total interaction is assumed to be dominantly electrostatic.⁴ The directionality of moderate and weak HBs is relatively soft but can still be identified with the orientation of electron lone pairs. A very important way⁴ of looking at HBs is to regard them as *incipient proton transfer reactions*, so that, in a stable HB, X-H...Y a partial bond H...Y is already established and the X-H bond is concomitantly weakened. In normal HBs the covalent X-H bond lengthens slightly but remains intact in the complex; if further proton-transfer occurs, the resulting complex becomes a H-bonded ion pair, the Y-H distance approaches the Y-H distance in the monomer cation, the X-H distance becomes much longer than the covalent X-H distance and the X-Y distance lengthens slightly.³ Interestingly, in a chain with 2 HBs both become stronger. This effect,

that is further amplified by considering chains of multiple HBs (as in the cyclic form of the hexamer water cluster) or an extended HB network (as in condensed phases of water, such as hexagonal ice), can be ascribed to σ -bond *cooperativity* since the charges flow through the X-H σ bonds leading to “polarization-enhanced H bonding”,⁴ and increased intermolecular orbital interactions.⁵

A long-standing controversy exists about the theoretical origins of H-bonding, whether primarily due to classical electrostatics (ionic or dipole-dipole forces) or quantum covalency (see, for instance refs. 6–10 and references therein). If the water HB is considered within the context of the complete range of molecular H bonding then it appears most probable that it is not solely electrostatic.⁹ A proton NMR resonance experiment¹¹ confirmed the covalency of HBs in liquid water and theoretical calculations⁵ showed that delocalized molecular orbitals exist in water rings.¹² Clearly, the interaction between two nuclei can be considered a true chemical bond only if there is a concentration of electron density around the internuclear axis. Results from recent theoretical and experimental investigations (in particular with Atomic Force Microscopy) suggest that the HB has both an electrostatic origin and a partly covalent character.¹³ Moreover, extensive investigations based on the “natural bond order” (NBO) method^{8,14} led to conclude that, although in HBs classical electrostatic effects are undoubtedly present, they seem to play only a secondary role with respect to non-classical resonance effects represented by intermolecular bond order or charge transfer.⁸ However, very recent studies cast doubts on the validity of the NBO method to evaluate charge-transfer effects in intermolecular interactions and hence on their predominance in characterizing the HBs.¹⁵ In any case their role in H bonding is probably not less significant than those of polarization and frozen density interactions.¹⁶

The prototypical HB in water dimer and HBs in the protonated water dimer, in other small molecules, in water cyclic clusters, and in ice, covering a wide range of bond strengths, are here theoretically investigated by first-principles calculations based on the Density Functional Theory (DFT). We compute structural, energetic, and electrostatic (induced molecular dipole moments) properties, also testing, in the water dimer case, hybrid and van-der-Waals corrected functionals. In particular, HBs are characterized in terms of differential electron density distributions and profiles, and of a geometric bonding parameter defined in terms of the positions of the centres of Maximally localized Wannier Functions. This parameter appears to be correlated to the Mayer bond order parameter and the HB strength, and

gives an estimate of the HB covalent character. By considering the cyclic water hexamer and the hexagonal phase of ice we also elucidate the importance of cooperative/anticooperative effects in H-bonding formation.

II. METHOD AND COMPUTATIONAL DETAILS

We perform first-principles calculations within the framework of the DFT. DFT represents the most popular theoretical method to investigate the structural and electronic properties of molecules and condensed matter systems from first principles, however the ability of DFT to quantitatively describe HBs between water molecules in either small clusters or the liquid state is not definitively assessed yet,^{17,18} although some Generalized Gradient Approximation (GGA) functionals, such as BLYP¹⁹ and PBE,²⁰ are commonly (and often successfully) used in DFT-based simulations of water, since they seem to offer a good compromise between computational efficiency and accuracy. In principle, long-range electron correlation interactions, attributed to van der Waals (vdW) forces, can contribute significantly to HB binding energies;^{21,22} however, vdW interactions are not properly described²³ by current GGA density functionals. Hence, in the conventional GGA descriptions of HBs, presumably electrostatic, exchange, and induction effects somehow compensate for the spurious or insufficient accounting of vdW long-range correlation forces.

Obviously, there is a strict relation between the electron density topology and physical-chemical properties and this can also be made more precise and quantitative by referring to the well-known DFT Hohenberg-Kohn theorem,²⁴ which asserts that the ground-state properties of a system are a consequence of its electron density. Therefore, we expect that, upon bonding, similar electron-charge redistributions basically correspond to the same type of interaction,²⁵ so that a detailed charge analysis represents a very useful tool for intermolecular-bonding characterization. To evaluate the electron density response due to the bond formation between different fragments we compute the *differential* charge density, $\Delta\rho$, defined as the difference between the total electron density of the system and the superposition of the densities of the separated fragments (atoms or molecules), keeping the same geometrical structure and atomic positions that these fragments have within the optimized system. This is a meaningful procedure since, for instance, the geometrical distortion of the two water molecules in a water dimer is insignificant.¹⁶ By drawing $\Delta\rho$ isosurfaces on

a planar plot we highlight the electron charge redistributions related to the HB formation. Moreover, one-dimensional profiles $\Delta\rho(z)$ can also be obtained, which are very effective for describing charge modifications upon H bonding: $\Delta\rho(z)$ is computed along an intermolecular z axis, as a function of z values, by integrating $\Delta\rho$ over the corresponding, orthogonal x, y planes.

We also rely on the use of the Maximally-Localized Wannier function (MLWF) formalism,²⁶ that allows the total electronic density to be partitioned, in a chemically transparent and unambiguous way, into individual fragment contributions. The MLWFs, $\{w_n(\mathbf{r})\}$, are generated by performing a unitary transformation in the subspace of the occupied Kohn-Sham orbitals, obtained by a standard DFT calculation, so as to minimize the total spread:

$$\Omega = \sum_n S_n^2 = \sum_n (\langle w_n | r^2 | w_n \rangle - \langle w_n | \mathbf{r} | w_n \rangle^2) . \quad (1)$$

Besides its spread, S_n , each MLWF is characterized also by its Wannier-function center (WFC), defined as the center of mass of the (square modulus) Wannier function. Note that, if spin degeneracy is exploited, every MLWF corresponds to 2 paired electrons. Knowledge of WFC positions also allows to estimate molecular dipole moments,²⁷ and the MLWFs can be even used to include vdW interactions in DFT.^{21,28}

Calculations have been performed mostly with the Quantum-ESPRESSO ab initio package²⁹ and the MLWFs have been generated as a post-processing calculation using the WanT package.³⁰ For our calculations on molecules and clusters we have adopted a periodically-repeated, simple cubic supercell, with a side of 16 Å, in such a way to make the interactions among periodic replicas negligible. Electron-ion interactions were described using ultrasoft pseudopotentials and the sampling of the Brillouin Zone was limited to the Γ -point. Instead for ice in the hexagonal phase we used an hexagonal supercell containing 12 water molecules at experimental density and with a $2 \times 2 \times 2$ k -point sampling of the Brillouin Zone.

III. RESULTS AND DISCUSSION

A. Water dimer

As can be seen looking at Fig. 1 and 2, showing the differential electron charge density, $\Delta\rho$, plotted on a 2D plane and integrated over x, y planes orthogonal to the intermolecular O-O z axis ($\Delta\rho(z)$ function), respectively, there is no overall electron-charge accumulation between the two O atoms of the water dimer in the optimal, linear HB configuration. Actually, one can only observe (see notation defined in Fig. 3) a small amount of electron-charge *redistribution*: an electron depletion of about $0.008 e$ (that is less than 1% of an electron) between the O atom of the *acceptor* molecule, O_a , and H (in the HB region) is exactly offset by an electron accumulation between H and the O atom of the *donor* molecule, O_d , while a more substantial (about $0.03 e$) charge transfer appears to occur from O_a to O_d . This is compatible with previous findings.^{8,16,31–34} The fact that the acceptor molecule contributes more than the donor is in line with the Lewis concept of acid/base behavior.³¹ As previously observed,³⁴ the amount of charge accumulated in the middle of the HB is 2 orders of magnitude smaller than in a typical covalent bond, such as, for instance, in the H_2 dimer, thus showing that in the water-dimer HB the electron pairing contribution is probably marginal and suggesting that instead charge polarization of one of the lone-pair orbital of the acceptor molecule towards the H atom of the donor molecule plays a key role.³⁴ Note also the pronounced electron-density depletion at the position of the H atom participating in the HB which therefore increases its positive charge.

Interestingly, Hartree-Fock (HF) methods do not give³⁴ strong evidence of charge transfer involving the lone pair orbital in contrast to results from DFT methods, in line with the substantial HF underbinding of the water dimer; instead DFT in different GGA flavors (such as PBE adopted here) accurately reproduces the water-dimer binding energy and bond length. In fact our PBE results for basic energetic and structural parameters of the optimal configuration of the water dimer (binding energy = -221 meV, O_a -H distance = 1.92 Å, H- O_d distance = 0.98 Å, O_a -H- O_d angle = 178° , H being the H atom involved in the HB) are in excellent agreement with literature reference data³⁵ (binding energy = -218 meV, O_a -H distance = 1.95 Å, H- O_d distance = 0.97 Å, O_a -H- O_d angle = 173°). From these considerations we expect that our analysis on redistributions of the electronic charge, at the

PBE level, is meaningful for a proper description of realistic H-bonded systems (particularly for water).

In Fig. 4 we report plots of $\Delta\rho(z)$ for the water dimer, obtained by DFT functionals different from PBE: vdW-DF-cx,^{36,37} which is one of the most recent versions of the vdW-DF family where vdW effects (not properly described by GGA functionals) are included by introducing DFT nonlocal correlation functionals, and PBE0³⁸ and B3LYP,³⁹ which are *hybrid* functionals where a given fraction of exact exchange is combined with the PBE or BLYP GGA functional, respectively: PBE0 is particularly accurate in describing H-bonding in water clusters,⁵ while B3LYP provides a better description of exchange in the intermolecular region than DFT approaches based on the GGA.⁴⁰ As can be seen, differential density profiles generated by these alternative functionals are very close to that obtained by PBE, so that also the amounts of the electronic charge redistributions are quite similar, thus showing that, for this system, vdW effects or inclusion or a fraction of exact exchange are not essential and PBE performs quite well, thus further confirming the previous considerations. The small impact of vdW interactions in moderate intermolecular HBs have been also recently reported.⁴¹

As a result of the electron-charge redistribution and polarization effects described above, the dipole moments of the acceptor and donor water molecules (estimated following ref. 27) are changed with respect to that of the single water molecule (*induced* dipole moments); moreover the dipole moment is slightly larger (2.18 D) for the acceptor molecule than for the donor one (2.00 D), the dipole moment of the isolated water molecule being 1.86 D. In particular, the larger dipole moment of the acceptor molecule originates from the small charge extrusion from O_a towards the H atom of the donor molecule (see Fig. 1). In summary, for the water dimer the nature of the HB can be characterized in terms of *quantum* effects associated to *redistribution* rather than transfer of electronic charge, in line with the conclusions of previous studies (see, for instance ref. 31): in fact a quantum description is required to describe the small deformations of the electron distributions of the water monomers when they interact, however the scenario is clearly different from that of a typical covalent bonds. In view of the above considerations, the success of semiempirical (often non-polarizable) models in reproducing many of the properties of water, that are obviously unable to properly describe charge-transfer and quantum-mechanical effects, appears to be to some extent fortuitous.³² A partial explanation for the good performances of these models,

despite the importance of charge transfer for the dimer, could be ascribed³² to the fact that charge transfer occurs for the H-bonded water dimer because there is an evident asymmetry between the two molecules as one donates and one accepts a HB, while in the condensed phases each molecule is in a more symmetric local environment.³² However, if symmetry is broken, for instance by the addition of a solute or the creation of an interface, then charge transfer would probably become more important and semiempirical models less reliable.³² For the sake of completeness, we should point out that water models exist (see, for instance, ref. 33), where the effects of charge transfer are included by adding an explicit H-bonding term.

In order to further characterize H-bonding in water dimer in terms of differential electron charge density, we have also studied what happens if the water-water distance is reduced (O-O distance = 2.5 Å) or increased (O-O distance = 4.0 Å) with respect to the equilibrium value (O-O distance = 2.91 Å), see curves in Fig. 5. One expects that decreasing the O-O distance would make the HB more covalent in character,³¹ while the covalent contribution and charge-transfer effects should be negligible at distances significantly larger than equilibrium.³² As can be seen, between O_a and the H atom involved in the H-bonding (that is in the HB region), at short water-water distance there is a more pronounced $\Delta\rho(z)$ depletion than at equilibrium distance, which does not support a H-bonding description in terms of covalent character but instead mainly a polarization mechanism, that is a process of separating opposite charges within the system; at the same time, more significant density accumulation takes place between H and O_d (that is in the covalent bond region) and in the region above O_d , while more pronounced density depletion is observed below O_a . Instead, at long water-water distance, in all the regions $\Delta\rho(z)$ is always quite reduced (note that, also in this case vdW effects do not seem to play a key role since replacing the PBE functional with vdW-DF-cx does not lead to significant changes).

B. Water hexamer, ice, and cooperativity

A special feature of the HB is its *cooperativity*, i.e., the fact that the local HB strength is influenced by the neighboring water molecules as a consequence of 3-body effects.⁴² In particular, a water molecule with 2 HBs whereit acts as both donor and acceptor is somewhat stabilized relative to one where it is either the donor or acceptor of 2 HBs,⁹ so that, for

instance, the formation of one HB in a H-bonded chain cooperatively enhances the strength of another HB. Both proton donor (D) and acceptor (A) participating in a H-bonding pair DA are capable of forming H bonding with the other water molecules; D can additionally accept two protons and donate one proton, and A can additionally donate two protons and accept one proton. A classification of H-bonding patterns considering the cooperativity has been proposed,⁴³ based on the parameter $d'a'DAd''a''$, where d and a are integers indicating the number of proton donors and acceptors to D (the *single prime*) and A (the *double prime*), respectively. Then, a magnitude given by $\text{MOH} = -d' + a' + d'' - a''$ has been introduced, assuming that each contribution for the enhanced ability of the HBs is the same and each effect is additive. The possible values for MOH are therefore: -2, -1, 0, 1, 2, 3, and 4. Note that HBs may not only enhance but also reduce the strengths of each other, which is probably responsible for the preferences of *homodromic* over *antidromic* cycles of HBs: in the preferred *homodromic* arrangement all HBs run in the same direction, while in the less common *antidromic* arrangement a change of orientation leads to local *anticooperativity*.^{4,44}

In order to investigate cooperative and anticooperative effects of H-bonding in water, we have studied two different conformations of the *cyclic* water hexamer (see Figs. 6 and 7). The first one is the usual *homodromic* configuration where all the HBs run in the same direction, leading to strong cooperative effects ($\text{MOH} = 2$ for all the HBs, which gives a total sum of 12), while, in the other *antidromic* one, some water molecules are rotated giving rise to an anticooperative effect ($\text{MOH} = 2$ for only 2 HBs, while $\text{MOH} = 0$ for the others, which gives a total sum of 4). The corresponding, integrated differential densities $\Delta\rho(z)$ are plotted in Fig. 8 where also the water-dimer profile is reported. For a proper comparison with the single HB of the dimer case of Fig. 2, $\Delta\rho(z)$ for the hexamers is obtained by choosing as the z axis the vertical axis of a *cylinder* centered around a selected O-O segment (connecting 2 adjacent water molecules) and with a radius of 2.3 Å (to essentially make differential-density contributions from other pairs of water molecules negligible); $\Delta\rho(z)$ is then obtained by integrating over planar regions orthogonal to z and contained inside the cylinder.

As can be seen, in the two water-hexamer cases the $\Delta\rho$ distribution looks quite different: in Fig. 6, for a given pair of water molecules, it resembles that of the water dimer shown in Fig. 1, while in Fig. 7 it becomes less symmetric (due to cooperative/anticooperative effects on different water molecule) and there is an appreciable accumulation in the HB

region only for those HBs that are characterized by nonzero MOH values ($\text{MOH} = 2$) and are located in the top-left and bottom-right regions of the hexagon. These observations are confirmed and made more quantitative by the $\Delta\rho(z)$ curves plotted in Fig. 8. In particular, the curve corresponding to the *homodromic* hexamer case is similar to that of the water dimer (see Fig. 2 and Fig. 5, particularly for the O-O distance shorter than at equilibrium), however, as expected, the cooperative effects tend to amplify the $\Delta\rho(z)$ fluctuations and charge redistributions; clearly in this configuration the distinction between O_d and O_a disappears since all the O atoms are simultaneously HB donors and acceptors. Instead, in the *antidromic* hexamer case, anticooperative effects tend to suppress $\Delta\rho(z)$ fluctuations and reduce charge redistributions (here the $\Delta\rho(z)$ profile is relative to the pair of water molecules on the left side of the hexagon shown in Fig. 7 and the bottom O atom is only acceptor while the top O atom is both donor and acceptor).

The “polarization-enhanced H bonding”⁴ due to cooperative effects can be quantitatively evaluated by computing the average HB energy E_b (defined as the water dimer or hexamer binding energy divided by the number of HBs, 1 or 6, respectively) and significantly affects also interatomic distances and dipole moments. In fact, $E_b = -221, -381, -228$ for the dimer, the *homodromic* hexamer and the *antidromic* hexamer, respectively. This means that cooperative effects in the favored cyclic hexamer configuration lead to an energy gain of more than 70% (note that similar effects are also observed in the ring structure of methanol hexamer⁴⁵). Instead, in the *antidromic* case cooperative effects are essentially suppressed and the absolute value of E_b is only marginally increased with respect to the water dimer case. As it is well known (see, for instance, ref. 42) cooperative effects are also revealed by the nearest neighbor O-O distances of H-bonded water molecules, whose average values are 2.90, 2.66, and 2.97 Å for the dimer, the *homodromic* hexamer and the *antidromic* hexamer, respectively (the corresponding HB O...H distances are $d_b = 1.92, 1.62, 1.92$ Å). Hence the O-O distance decrease with respect to the dimer provides direct evidence for cooperativity in *homodromic* hexamer,³ and confirms that, for a given substance such as water, shorter O-O (and O...H) distances generally correspond to stronger HBs.

HB cooperativity also leads to a significant enhancement of the water-molecule dipole moments as a consequence of polarization effects; in fact, the average dipole-moment values are 2.09, 3.05, 2.31 D for the dimer, the *homodromic* hexamer and the *antidromic* hexamer, respectively (we remember that the dipole moment of the isolated water molecule is 1.86

D). Hence, in the *homodromic* hexamer there is a dipole increase of almost 50% with respect to the dimer case (and of more than 60% with respect to the isolated water molecule), while in the *antidromic* case the dipole increase is considerably reduced (about 10%). These findings on cyclic water structures are important also because the exploration of structural and bonding properties of small water clusters provides a key for understanding anomalous properties of water in the liquid and solid phases.⁴³

We have also investigated the case of ice in the standard *hexagonal* phase, where, in the ideal structure, all the HBs are characterized by $\text{MOH} = 2$, thus suggesting again substantial cooperative effects. As can be seen in Fig. 8 (two-dimensional plots for HBs in ice are not reported since they closely resemble those relative to water dimer and cyclic hexamer), the $\Delta\rho(z)$ profile turns out to be intermediate between that of water dimer and that of *homodromic* hexamer and the same is true for the HB energy: $E_b = -328$ meV. Note however, that in the ice case the average water-molecule dipole moment is 3.36 D, which is even larger than in the *homodromic* hexamer (3.05 D). This substantial induced dipole moment can be ascribed to pronounced polarization effects due to the presence of neighbor water molecules within the 3-dimensional ice network.

C. Protonated water dimer

The protonated water dimer H_5O_2^+ plays an important role in the kinetics of aqueous solutions as well as in atmospheric chemistry.⁴⁶ This system is characterized by a relatively flat potential energy surface: in the global minimum, $\text{H}_2\text{O}-\text{H}^+-\text{H}_2\text{O}$, the midpoint H nucleus, which bridges the two water molecules, is centered approximately 1.2 Å from each of the O atoms; however, there is another stationary point on the potential energy surface, $\text{H}_2\text{O}\dots\text{H}^+-\text{H}_2\text{O}$, whose energy is only about 0.4 kcal/mol ($= 0.02$ eV) higher than the global minimum, where the midpoint H nucleus is slightly closer to one of the O atoms.⁴⁶ The former, most stable, $\text{H}_2\text{O}-\text{H}^+-\text{H}_2\text{O}$ configuration can be described as obtained by the formation of 2 symmetric covalent bonds (*Zundel cation*), while the latter, $\text{H}_2\text{O}\dots\text{H}^+-\text{H}_2\text{O}$, is characterized by one HB and one covalent bond.

Although the two different configurations are almost isoenergetic, their differential electron charge densities (see Figs. 9 and 10) and $\Delta\rho(z)$ profiles (shown in Fig. 11, where also the dimer curve is reported for comparison) look quite different: in fact, the curve of

Fig. 11, relative to $\text{H}_2\text{O}\dots\text{H}^+-\text{H}_2\text{O}$, qualitatively resembles that of water dimer, but with much larger charge fluctuations, while $\Delta\rho(z)$ for $\text{H}_2\text{O}-\text{H}^+-\text{H}_2\text{O}$ exhibits a single pronounced maximum (typical of conventional covalent bonds) centered around the midpoint H nucleus. $\text{H}_2\text{O}\dots\text{H}^+-\text{H}_2\text{O}$ is of particular interest because it can be considered as a *strong* HB, being characterized by a binding energy of about 1.5 eV,⁴ which is almost an order of magnitude larger than that of the ordinary water-dimer HB. Note that also the $\text{O}\dots\text{H}^+$ distance is much shorter, 1.31 Å, than that of $\text{O}\dots\text{H}$ in water dimer, 1.92 Å.

D. HB characterization

The prototypical HB in water dimer and HBs in other systems, corresponding to wide range of bond strengths, can also be quantitatively characterized by a single geometric bonding parameter, CCP, that is found to be correlated to the Mayer bond order (MBO) parameter.^{47,48} The MBO concept represents a popular tool to obtain insight into the strength and nature of bonding from first-principles calculations because takes all the contributions to the bond into account, although it is not devoid of limitations (see, for instance, ref. 49). We have explicitly computed MBO parameters for the systems investigated in the present study using the ab initio CPMD package.⁵⁰

The *covalent character* parameter, CCP, is based on the positions (and their changes upon bonding) of the centres, WFCs, of the MLWFs generated from the Kohn-Sham orbitals (see Method section) and can be considered as an extrapolation of a concept already introduced in the seminal paper of Marzari and Vanderbilt²⁶ for the characterization of the *ionic* bonding: “... the shift of the Wannier center away from the bond center might serve as a kind of measure of bond ionicity.” For instance, given our pseudopotential approximation, for a single water molecule we explicitly consider 8 valence electrons, the 2 additional oxygen-core electrons being essentially inert from the point of view of the bonding properties. Due to spin degeneracy we need therefore to consider 4 doubly-occupied MLWFs and their relative WFCs. These WFCs are tetrahedrally oriented, and two of them describe the lone-pair orbitals while the other two represent covalent-bond orbitals (see Fig. 3).²⁷ We also point out that, particularly in weak and moderate HBs, the MLWF spreads are hardly affected by bonding, which represents a justification to focus on WFCs positions only: in fact, in the case of the water dimer, the spread of the MLWF involved in the HB is changed by only

0.3% from the value of the corresponding, lone-pair MLWF of the isolated water molecule, and, even in hexagonal ice, the variation is smaller than 3%.

By considering, as the reference system, always the water dimer investigated above (the generalization to other H-bonded systems is easy) and referring to the schematic, explanatory Fig. 3, in order to characterize the HB between O_a and H, we propose the following definition for the CCP parameter:

$$\text{CCP} = (l - l_0)/(d_m - l_0) , \quad (2)$$

where l and l_0 denote the distances of the W_l WFC from O_a in the H-bonded system and in the isolated water molecule, respectively, and $d_m = d_b/2$ is half the HB distance between O_a and H.

Note that, on the basis of the density-differential analysis reported above, we expect that W_l is pulled out due to the formation of the HB, so that $l > l_0$ (the same behavior is also observed in liquid water²⁷). Basically, according to this definition, CCP varies from 0 to 1: in the limiting cases, CCP= 0 (zero covalent contribution) if $l = l_0$, that is the distance of W_l from O_a is not changed upon bonding, while CCP= 1 (100% covalent contribution) if $l = d_m$, so that W_l , which indicates the center-of-mass position of the interfragment electron charge, is precisely located at the geometric (midpoint) bond center, as, for instance, in the H dimer, H_2 . Therefore our CCP represents indeed a simple estimate of the HB covalent character, although it should be pointed out that a unique and commonly accepted definition of covalent contribution in a HB is still missing, so that the HB covalency of water dimer has been given different weights, depending on the different theoretical frameworks and definitions adopted (see, for instance ref. 10 and references therein).

In Table I we report the CCP values for different systems (including those discussed above) covering a wide range of bond strengths, together with the corresponding MBO parameter, the HB energy, E_b , and bond length, d_b . As far as the water dimer is concerned, at the equilibrium distance CCP=0.02, so that the covalent contribution (2.0 %) turns out to be rather small; it is much smaller (essentially negligible) in the less favored, *cyclic* and *bifurcated* water-dimer conformations, and when the intermolecular distance is longer (O_a - O_a separation=4.0 Å) than the equilibrium one. Interestingly, the 4.0 Å distance has been indicated in the literature as the cutoff distance when any covalent contribution vanishes.^{6,10} In line with the differential-density analysis reported above, even at intermolecular distance

shorter (O_a-O_d separation=2.5 Å) than the equilibrium one, the covalent contribution is not much increased (2.5 %). Even for the HB in the methane-water compound (CH_4-H_2O) covalency appears to be marginal. As expected, for the cyclic water hexamer in the *homodromic* configuration, the CCP value (averaged over the 6 HBs) is much larger than the corresponding values both for the *antidromic* structure and for the water dimer, thus showing that in this case the covalent contribution is much more pronounced, again in agreement with the behavior of the differential-density profiles and with the cooperative effects discussed above. CCP for ice in the hexagonal phase is comparable to that of the cyclic water hexamer in the *homodromic* configuration. The CCP values for the methanol dimer (CH_3OH-CH_3OH) and for the methanol hexamer ($((CH_3OH)_6)$) in the *ring* structure are very close to those for the water dimer and water hexamer, respectively, in line with the behavior of the corresponding HB binding energies. Note that methanol rings have been proposed⁴⁵ as good examples to illustrate the covalent contribution to the HB.

Finally, the relatively high CCP values for $H_2O...H^+-H_2O$ and $FH-F^-$, which represent *strong* H-bonded systems (their HB energy is almost an order of magnitude larger than that of the water dimer), lead us to conclude that these complexes certainly possess substantial covalent character; in fact, they are sometimes considered as a chemically bound species.^{3,8} Note that, for the Zundel cation $H_2O-H^+-H_2O$, CCP=0.357, thus confirming the pronounced covalency of this system, as also discussed in the previous subsection.

Data in Table I clearly show that there is a high correlation among the listed quantities. In particular the *correlation coefficient* between E_b and d_b is 0.68, between E_b and MBO is -0.89, between E_b and CCP is -0.94, and between MBO and CCP is 0.94, thus pointing out that, particularly MBO and CCP are strictly correlated, but CCP better correlates with E_b than MBO. Hence this simple geometric parameter, based on variations of the WFCs positions, can be used to characterize a wide range of bond strengths, where electrostatic, covalent, and dispersion contributions largely vary in their relative weights.

In Table II we report the values of MBO and CCP for the $H_2O...H^+-H_2O$ system at different HB lengths, starting from the equilibrium O-O d_{OO} distance to larger distances (the geometry of the system is relaxed at fixed d_{OO} distance). In this case the correlation coefficient between E_b and d_b is 0.94, between E_b and MBO is -0.99, between E_b and CCP is -0.84, and between MBO and CCP is 0.89, thus confirming again the high correlation between MBO and CCP even away from equilibrium.

IV. CONCLUSIONS

The prototypical HB in water dimer and HBs in the protonated water dimer, in other small molecules, in water cyclic clusters, and in ice, covering a wide range of bond strengths have been investigated in terms of different structural, energetic, and electrostatic (induced molecular dipole moments) properties and particularly focusing on the differential electron density and on the shifts of the centres of the MLWFs. The information from the latter quantities can be conveyed into a single geometric bonding parameter, CCP, that appears to be correlated to the MBO and the HB strength, and gives an estimate of the HB covalent character. For HBs in water (dimer, hexamers, ice) and methanol CCP ranges from 0.00 to 0.11 (MBO from 0.01 to 0.23), thus leading to the conclusion that, for such moderate HBs, the covalent contribution is present but not predominant. Test calculations on water dimer show that, at least for moderate-strength HBs, using the standard PBE functional is appropriate since adopting alternative DFT functionals that include vdW effects or are hybrid in character only leads to small effects. By considering the cyclic water hexamer and the hexagonal phase of ice we have also elucidated the importance of cooperative/anticooperative effects in H-bonding formation.

-
- ¹ G. A. Jeffrey, *An Introduction to Hydrogen bonding*, Oxford University Press, New York (1997).
- ² G. E. Walrafen, M. R. Fisher, M. S. Hokmabadi, W.-H. Yang, *J. Chem. Phys.* **85**, 6970 (1986).
- ³ A. D. Buckingham, J. E. Del Bene, S. A. C. McDowell, *Chem. Phys. Lett.* **463**, 1 (2008).
- ⁴ T. Steiner, *Angew. Chem. Int. Ed.* **41**, 48 (2002).
- ⁵ B. Wang, M. Xin, X. Dai, R. Song, Y. Meng, J. Han, W. Jiang, Z. Wang, R. Zhang, *Phys. Chem. Chem. Phys.* **17**, 2987 (2015); B. Wang, L. Wang, X. Dai, Y. Gao, W. Jiang, J. Han, Z. Wang, R.-Q. Zhang, *Int. J. Quantum Chem.* **115**, 817 (2015).
- ⁶ E. Isaacs, A. Shukla, P. Platzman, D. Hamann, B. Barbiellini, C. Tulk, *Phys. Rev. Lett.* **82**, 600 (1999); B. Barbiellini, A. Shukla, *Phys. Rev. B* **66**, 235101 (2002).
- ⁷ A. H. Romero, P. L. Silvestrelli, M. Parrinello, *J. Chem. Phys.* **115**, 115 (2001).
- ⁸ F. Weinhold, R. A. Klein, *Mol. Phys.* **110**, 565 (2012).
- ⁹ M. F. Chaplin, *Water’s hydrogen bond strength*, In: *Water and Life*, ed. R. M. Lynden-Bell, S.

- Conway Morris, J. D. Barrow, J. L. Finney and C. L. Harper, Jr. (CRC Press, Boca Raton, 2010) pp 69-86; arXiv:0706.1355 (2007).
- ¹⁰ F. Sterpone, L. Spanu, L. Ferraro, S. Sorella, L. Guidoni, J. Chem. Theory Comput. **4**, 1428 (2008).
 - ¹¹ H. Elgabarty, R. Z. Khaliullin, T. D. Kühne, Nature Communications **6**, 8318 (2015).
 - ¹² B. Wang, W. Jiang, X. Dai, Y. Gao, Z. Wang, R.-Q. Zhang, Scientific Reports **6**, 22099 (2016).
 - ¹³ J. Zhang, P. Chen, B. Yuan, W. Ji, Z. Cheng, X. Qiu, Science **342**, 611 (2013).
 - ¹⁴ A. E. Reed, F. Weinhold, L. A. Curtiss, D. J. Pochatko, J. Chem. Phys. **84**, 5687 (1986).
 - ¹⁵ A. J. Stone, J. Phys. Chem. A **121**, 1531 (2017).
 - ¹⁶ R. Z. Khaliullin, E. A. Cobar, A. T. Bell, M. Head-Gordon, J. Phys. Chem. A **111**, 8753 (2007); R. Z. Khaliullin, A. T. Bell, M. Head-Gordon, J. Chem. Phys. **128**, 184112 (2008).
 - ¹⁷ B. Santra, A. Michaelides, M. Scheffler, J. Chem. Phys. **127**, 184104 (2007).
 - ¹⁸ B. Santra, A. Michaelides, M. Fuchs, A. Tkatchenko, C. Filippi, M. Scheffler, J. Chem. Phys. **129**, 194111 (2008).
 - ¹⁹ A. D. Becke, Phys. Rev. A **38**, 3098 (1988); C. Lee, W. Yang, R. C. Parr, Phys. Rev. B **37**, 785 (1988).
 - ²⁰ J. P. Perdew, K. Burke, M. Ernzerhof, Phys. Rev. Lett. **77**, 3865 (1996).
 - ²¹ P. L. Silvestrelli, Chem. Phys. Lett. **475**, 285 (2009).
 - ²² J. S. Arey, P. C. Aeberhard, I.-C. Lin, U. Rothlisberger, J. Phys. Chem. B **113**, 4726 (2009).
 - ²³ See, for instance, W. Kohn, Y. Meir, D. E. Makarov, Phys. Rev. Lett. **80**, 4153 (1998).
 - ²⁴ P. Hohenberg, W. Kohn, Phys. Rev. **136**, B864 (1964).
 - ²⁵ J. R. Lane, J. Contreras-García, J. P. Piquemal, B. J. Miller, H. G. Kjaergaard, J. Chem. Theory Comput. **9**, 3263 (2013).
 - ²⁶ N. Marzari, D. Vanderbilt, Phys. Rev. B **56**, 12847 (1997).
 - ²⁷ P. L. Silvestrelli, M. Parrinello, Phys. Rev. Lett. **82**, 3308 (1999); J. Chem. Phys. **111**, 3572 (1999).
 - ²⁸ P. L. Silvestrelli, Phys. Rev. Lett. **100**, 053002 (2008); J. Phys. Chem. A **113**, 5224 (2009).
 - ²⁹ P. Giannozzi, S. Baroni, N. Bonini, M. Calandra, R. Car, C. Cavazzoni, D. Ceresoli, G. L. Chiarotti, M. Cococcioni, I. Dabo, A. Dal Corso, S. Fabris, G. Fratesi, S. de Gironcoli, R. Gebauer, U. Gerstmann, C. Gougoussis, A. Kokalj, M. Lazzeri, L. Martin-Samos, N. Marzari, F. Mauri, R. Mazzarello, S. Paolini, A. Pasquarello, L. Paulatto, C. Sbraccia, S. Scandolo, G.

- Sclauzero, A. P. Seitsonen, A. Smogunov, P. Umari, R. M. Wentzcovitch, *J. Phys.: Condens. Matter* **21**, 395502 (2009); <http://arxiv.org/abs/0906.2569>.
- ³⁰ WanT code by A. Ferretti, B. Bonferroni, A. Calzolari, and M. Buongiorno Nardelli, <http://www.wannier-transport.org> ; see also A. Calzolari, N. Marzari, I. Souza, M. Buongiorno Nardelli, *Phys. Rev. B* **69**, 035108 (2004).
- ³¹ O. Gálvez, P. C. Gómez, L. F. Pacios, *J. Chem. Phys.* **115**, 11166 (2001).
- ³² A. J. Lee, S. W. Rick, *J. Chem. Phys.* **134**, 184507 (2011).
- ³³ H. Jiang, O. A. Moulτος, I. G. Economou, A. Z. Panagiotopoulos, *J. Phys. Chem. B* **120**, 12538 (2016).
- ³⁴ A. Nilsson, H. Ogasawara, M. Cavalleri, D. Nordlund, M. Nyberg, Ph. Wernet, L. G. M. Pettersson, *J. Chem. Phys.* **122**, 154505 (2005).
- ³⁵ G. S. Tschumper, M. L. Leininger, B. C. Hoffman, E. F. Valeev, H. F. Schaefer III, M. Quack, *J. Chem. Phys.* **116**, 690 (2002).
- ³⁶ K. Berland, P. Hyldgaard, *Phys. Rev. B* **89**, 035412 (2014).
- ³⁷ K. Berland, C. A. Arter, V. R. Cooper, K. Lee, B. I. Lundqvist, E. Schröder, T. Thonhauser, P. Hyldgaard, *J. Chem. Phys.* **140**, 18A539 (2014).
- ³⁸ C. Adamo, V. Barone, *J. Chem. Phys.* **110**, 6158 (1999).
- ³⁹ A. D. Becke, *J. Chem. Phys.* **98**, 5648 (1993); P. J. Stephens, F. J. Devlin, C. F. Chabalowski, M. J. Frisch, *J. Phys. Chem.* **98**, 11623 (1994).
- ⁴⁰ F. Fuster, B. Silvi, *Theor. Chem. Acc.* **104**, 13 (2000).
- ⁴¹ S. A. Katsyuba, M. V. Vener, E. E. Zvereva, J. G. Brandenburg, *Chem. Phys. Lett.* **672**, 124 (2017).
- ⁴² C. Pérez, D. P. Zaleski, N. A. Seifert, B. Temelso, G. C. Shields, Z. Kisiel, B. H. Pate, *Angew. Chem. Int. Ed.* **53**, 14368 (2014).
- ⁴³ K. Ohno, M. Okimura, N. Akai, Y. Katsumoto, *Phys. Chem. Chem. Phys.* **7**, 3005 (2005).
- ⁴⁴ W. Saenger, *Nature* **279**, 343 (1979).
- ⁴⁵ S. Kashtanov, A. Augustson, J.-E. Rubensson, J. Nordgren, H. Ågren, J.-H. Guo, Y. Luo, *Phys. Rev. B* **71**, 104205 (2005).
- ⁴⁶ J. Dolenc, J. Koller, *Acta Chim. Slov.* **53**, 229 (2006).
- ⁴⁷ I. Mayer, *Chem. Phys. Lett.* **97**, 270 (1983).
- ⁴⁸ A. J. Bridgeman, G. Cavigliasso, L. R. Ireland, J. Rothery, *J. Chem. Soc., Dalton Trans.* 2095

(2001).

⁴⁹ P. Szarek, Y. Sueda, A. Tachibana, J. Chem. Phys. **129**, 094102 (2008).

⁵⁰ <http://www.cpmc.org/>

TABLE I: HB energy, E_b , bond length, d_b , MBO and CCP parameters, for different H-bonded systems, listed in order of increasing MBO values. $\text{H}_2\text{O}-\text{H}_2\text{O}-2.5\text{\AA}$ and $\text{H}_2\text{O}-\text{H}_2\text{O}-4.0\text{\AA}$ indicate the water dimer at O-O distances shorter and longer than the equilibrium one, $\text{H}_2\text{O}-\text{H}_2\text{O}-cyc$ and $\text{H}_2\text{O}-\text{H}_2\text{O}-bif$ the *cyclic* and *bifurcated*, less favored water-dimer conformations, $(\text{H}_2\text{O})_6-homo$ and $(\text{H}_2\text{O})_6-anti$ the water hexamer in the *homodromic* and *antidromic* structures, and $\text{H}_2\text{O}-ice-hex$ ice in the hexagonal phase.

system	$E_b(\text{meV})$	$d_b(\text{\AA})$	MBO	CCP
$\text{H}_2\text{O}-\text{H}_2\text{O}-4.0\text{\AA}$	-89	3.02	0.010	0.003
$\text{H}_2\text{O}-\text{H}_2\text{O}-cyc$	-81	2.33	0.019	0.006
$\text{CH}_4-\text{H}_2\text{O}$	-25	2.59	0.021	0.003
$\text{H}_2\text{O}-\text{H}_2\text{O}-bif$	-68	2.54	0.022	0.004
$\text{H}_2\text{O}-\text{H}_2\text{O}$	-221	1.92	0.105	0.020
$(\text{H}_2\text{O})_6-anti$	-228	1.92	0.124	0.040
$\text{CH}_3\text{OH}-\text{CH}_3\text{OH}$	-232	1.89	0.124	0.041
$\text{H}_2\text{O}-\text{H}_2\text{O}-2.5\text{\AA}$	-74	1.54	0.182	0.025
$\text{H}_2\text{O}-ice-hex$	-328	1.75	0.191	0.083
$(\text{H}_2\text{O})_6-homo$	-381	1.62	0.222	0.105
$(\text{CH}_3\text{OH})_6$	-389	1.59	0.226	0.105
$\text{H}_2\text{O}\dots\text{H}^+-\text{H}_2\text{O}$	-1651	1.31	0.366	0.172
$\text{FH}-\text{F}^-$	-1969	1.16	0.421	0.290

TABLE II: O-O distance, d_{OO} , bond length, d_b , HB energy, E_b , MBO and CCP parameters for the $\text{H}_2\text{O}\dots\text{H}^+-\text{H}_2\text{O}$ system, at different d_{OO} distances.

d_{OO} (Å)	d_b (Å)	E_b (meV)	MBO	CCP
2.38	1.31	-1651	0.366	0.172
2.65	1.55	-1458	0.298	0.056
2.91	1.87	-1154	0.196	0.044
3.18	2.16	-903	0.126	0.027
3.44	2.44	-714	0.078	0.016
3.70	2.71	-573	0.046	0.015
3.97	2.98	-468	0.026	0.011
4.23	3.24	-389	0.014	0.002
5.29	4.31	-208	0.001	0.003

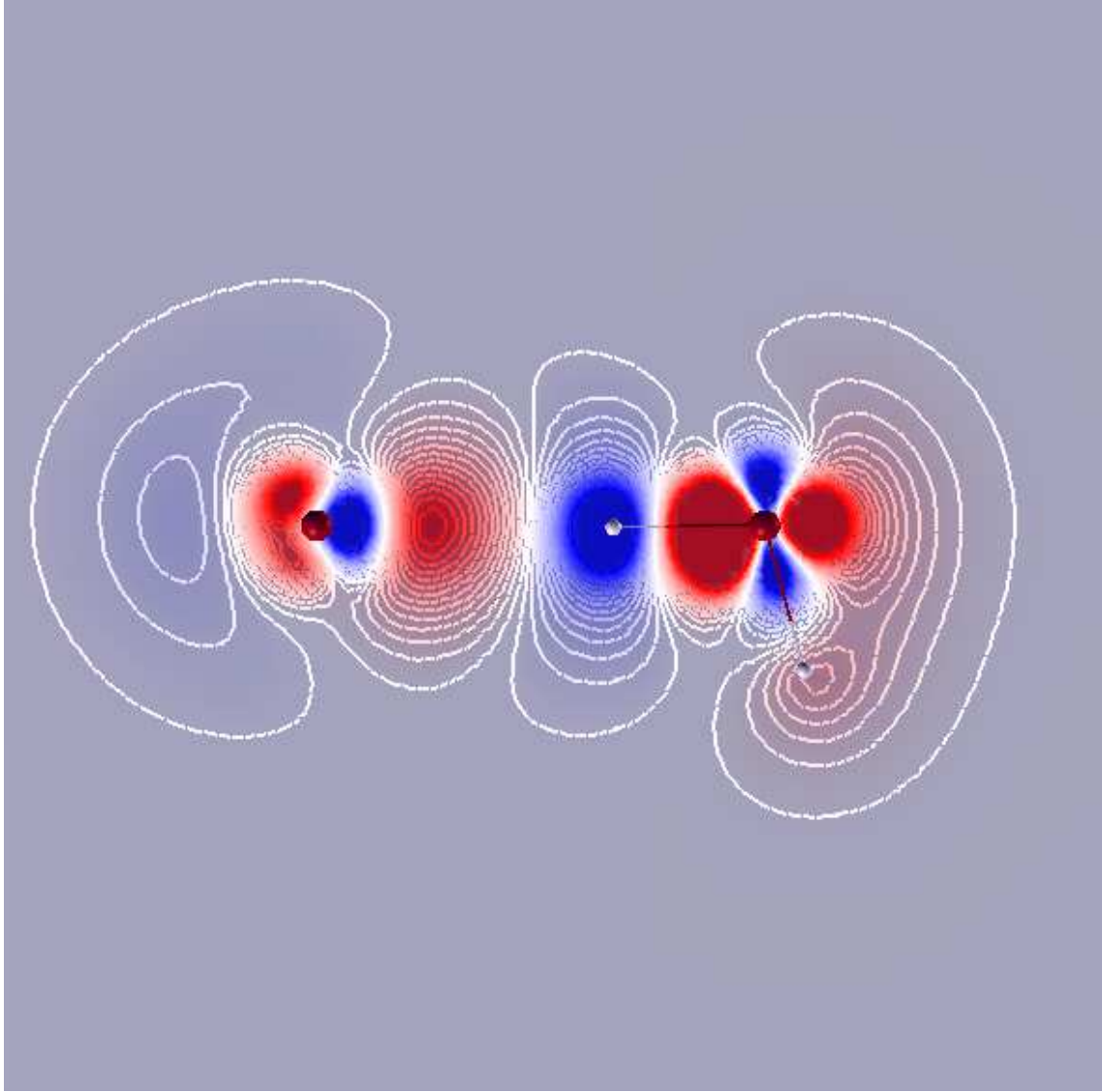


FIG. 1: Differential electron charge density, $\Delta\rho$, for the water dimer in the optimal, linear HB configuration (shown is the difference between the dimer density and those of the isolated water molecules), plotted on a plane containing the HB. The red and white balls denote O and H atoms, respectively. Red areas indicate electron density gain, while blue areas indicate loss of electron density; increments between contour lines correspond to $2 \times 10^{-4} e/\text{\AA}^3$ (within the range $\pm 0.003 e/\text{\AA}^3$).

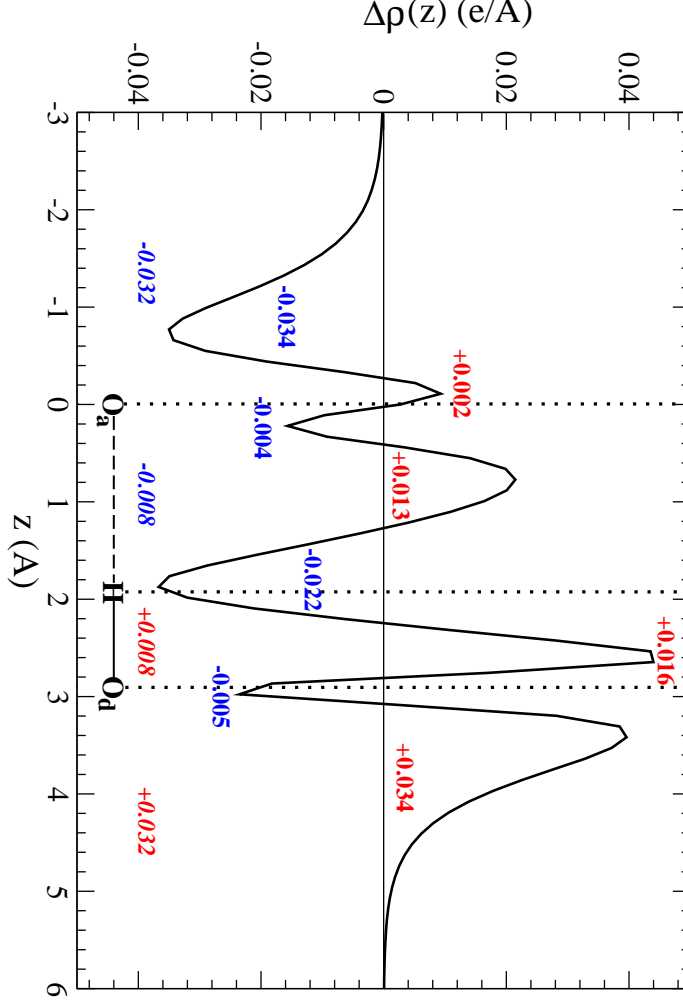


FIG. 2: Differential electron charge density, along the z axis, $\Delta\rho(z)$, integrated over x, y planes (see text for the definition) for the water dimer in the optimal, linear HB configuration (corresponding to Fig. 1) Positive (in red) and negative (in blue) numerical values inside or near the peaks indicate the corresponding electron charge (in e) obtained by integral of $\Delta\rho(z)$ along z ; the numerical values in italics in the bottom indicate the electron charge below the O atom of the *acceptor* molecule O_a , between O_a and H (the HB region), between H and O_d (the covalent bond region), and above the O atom of the *donor* molecule O_d , respectively (these 4 regions are delimited by vertical, dotted lines).

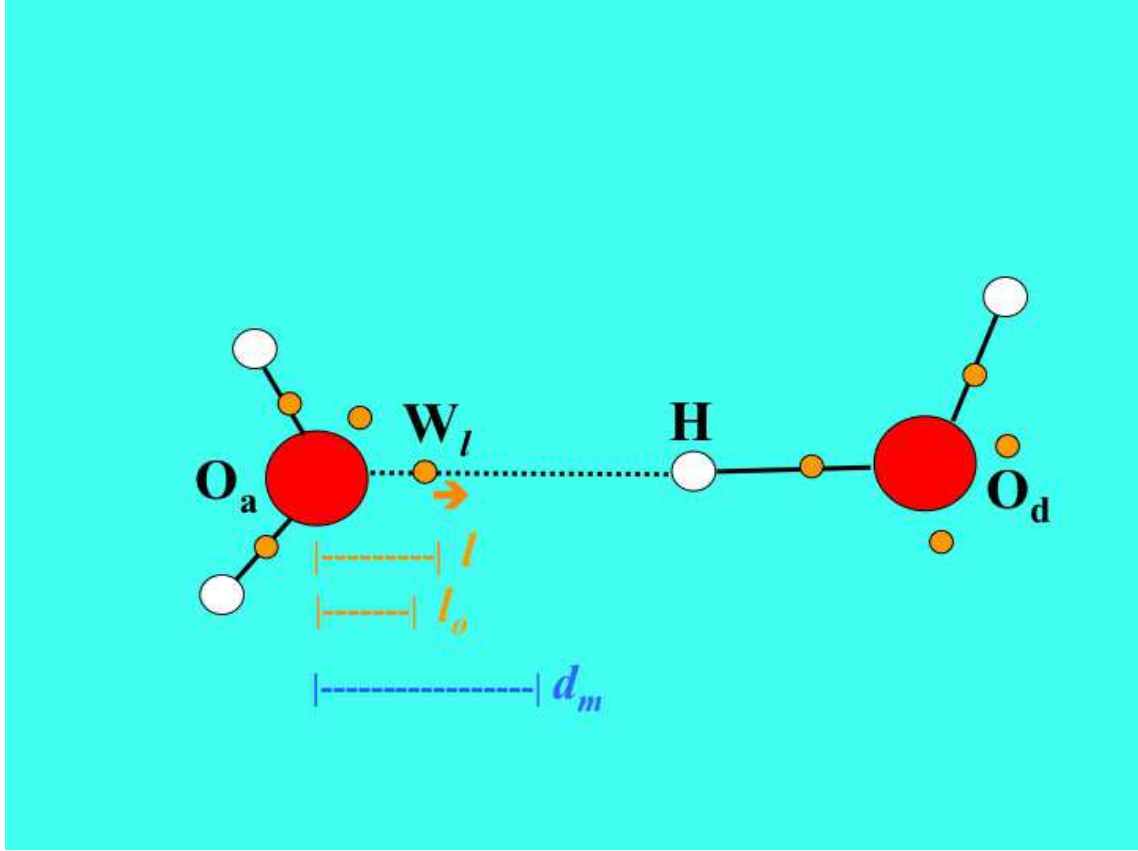


FIG. 3: Explanatory figure with schematic distributions of atoms (red balls: O atoms of the donor, O_d , and acceptor, O_a , molecule; white balls: H atoms) and WFCs (orange balls) involved in the definitions of the CCP parameter (see text), for the water dimer.

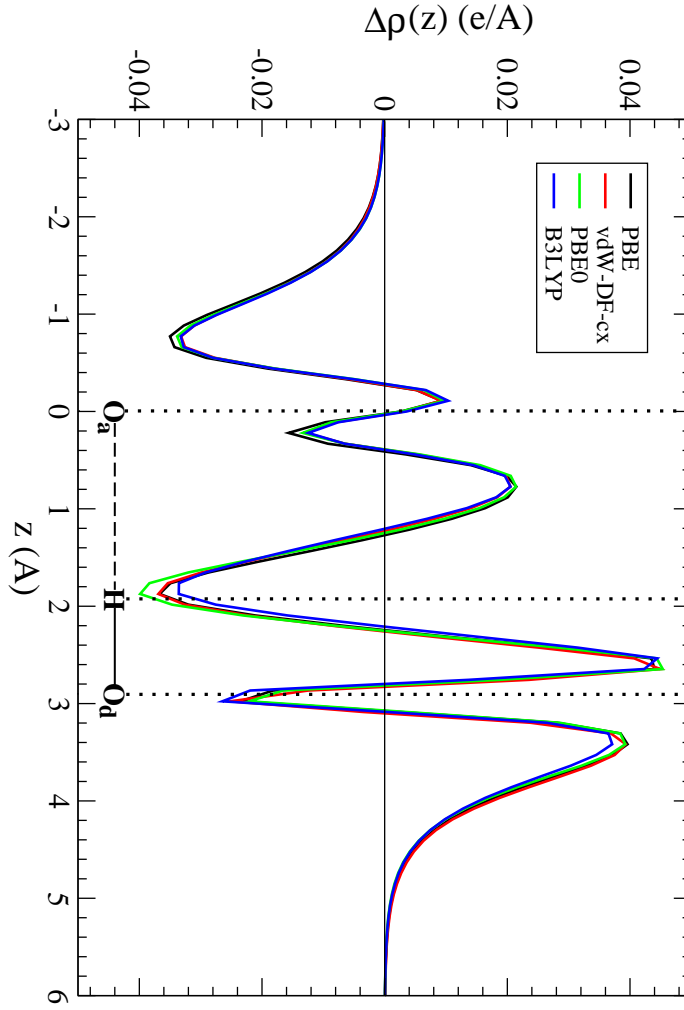


FIG. 4: Differential electron charge density, along the z axis, $\Delta\rho(z)$, integrated over x, y planes (see Fig. 2) obtained using different DFT functionals: PBE (GGA), vdW-DF-cx (vdW-corrected DFT), and two hybrid functionals, PBE0 and B3LYP.

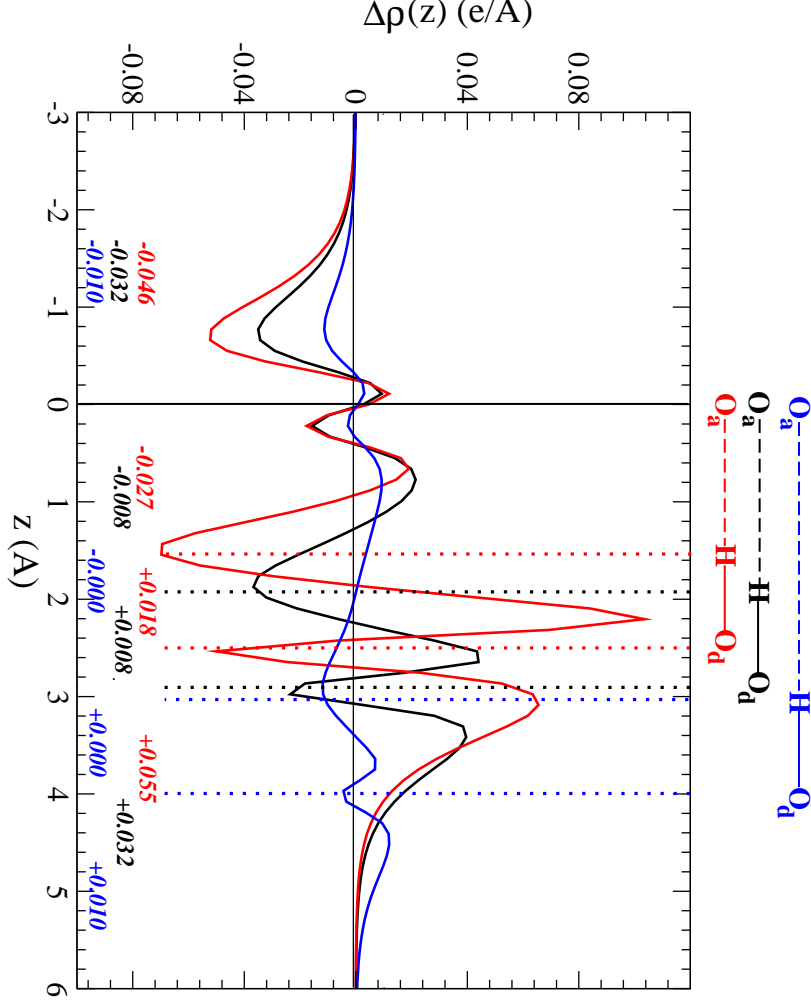


FIG. 5: Differential electron charge density, along the z axis, $\Delta\rho(z)$, integrated over x, y planes (see Fig. 2) obtained at PBE level and considering a water-water distance shorter (O-O distance = 2.5 Å, red curve) or longer (O-O distance = 4.0 Å, blue curve) than the equilibrium value (O-O distance = 2.91 Å, black curve). Positive and negative numerical values indicate the electron charge (in e) below the O atom of the *acceptor* molecule O_a , between O_a and H (the HB region), between H and O_d (the covalent bond region), and above the O atom of the *donor* molecule O_d , respectively (these 4 regions are delimited by vertical, dotted lines).

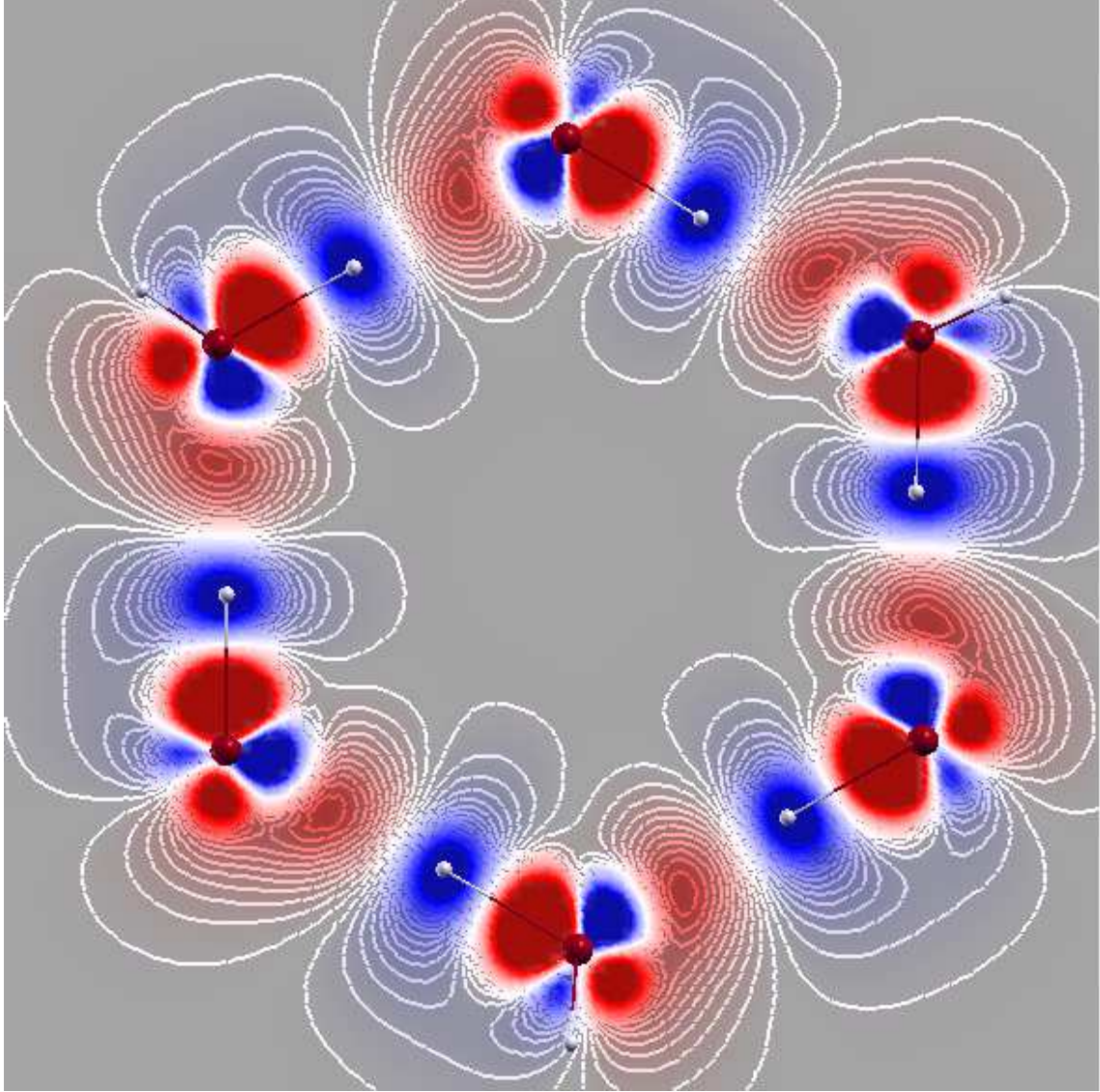


FIG. 6: Differential electron charge density, $\Delta\rho$, for the water hexamer in the cyclic *homodromic* configuration (shown is the difference between the dimer density and those of the isolated water molecules), plotted on a plane containing the hexamer ring and the HBs. The red and white balls denote O and H atoms, respectively. Red areas indicate electron density gain, while blue areas indicate loss of electron density; increments between contour lines correspond to $7 \times 10^{-4} e/\text{\AA}^3$ (within the range $\pm 0.01 e/\text{\AA}^3$).

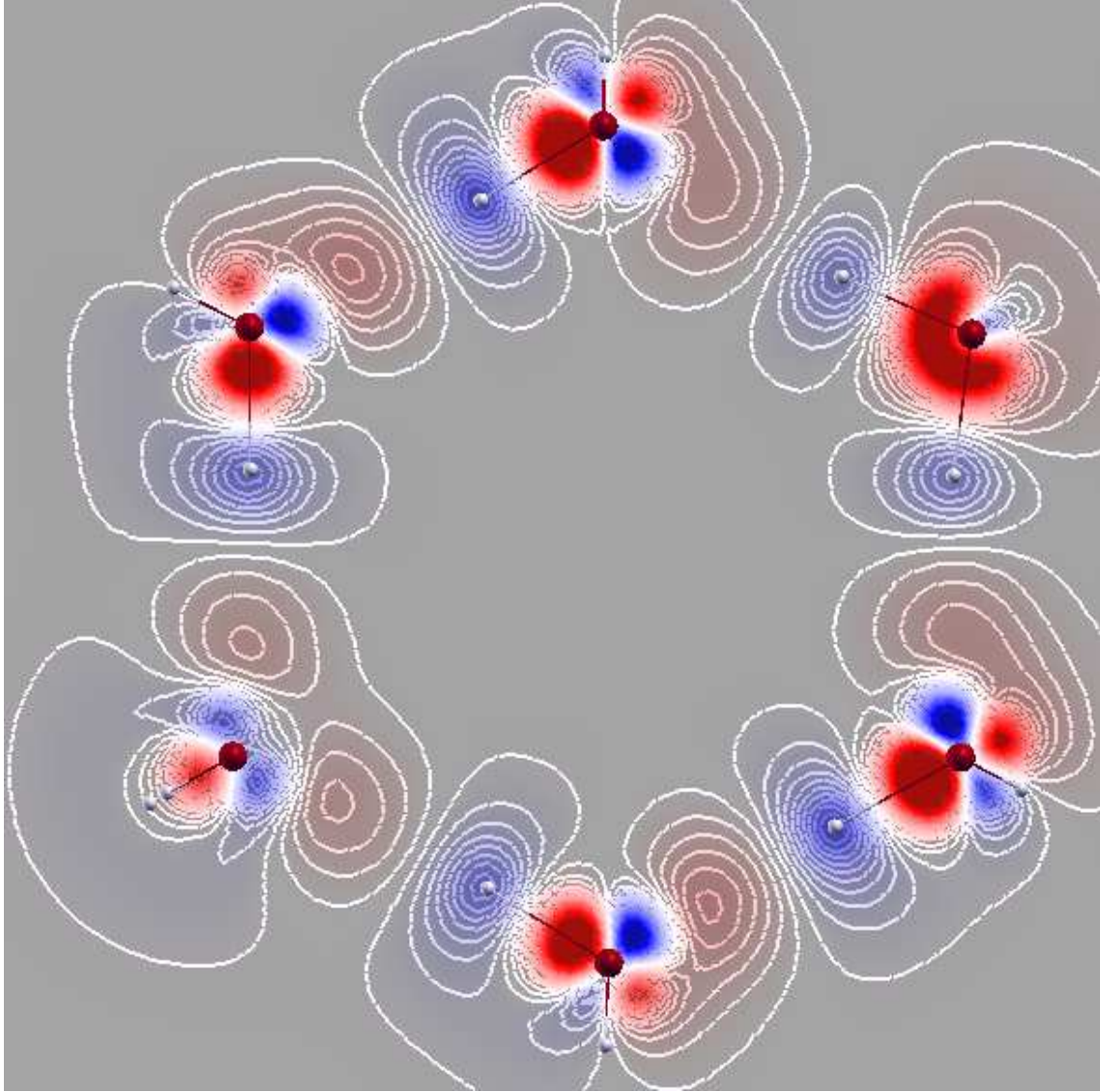


FIG. 7: Differential electron charge density, $\Delta\rho$, for the water hexamer in the cyclic *antidromic* configuration (shown is the difference between the dimer density and those of the isolated water molecules), plotted on a plane containing the hexamer ring and the HBs. The red and white balls denote O and H atoms, respectively. Red areas indicate electron density gain, while blue areas indicate loss of electron density; increments between contour lines correspond to $7 \times 10^{-4} e/\text{\AA}^3$ (within the range $\pm 0.01 e/\text{\AA}^3$).

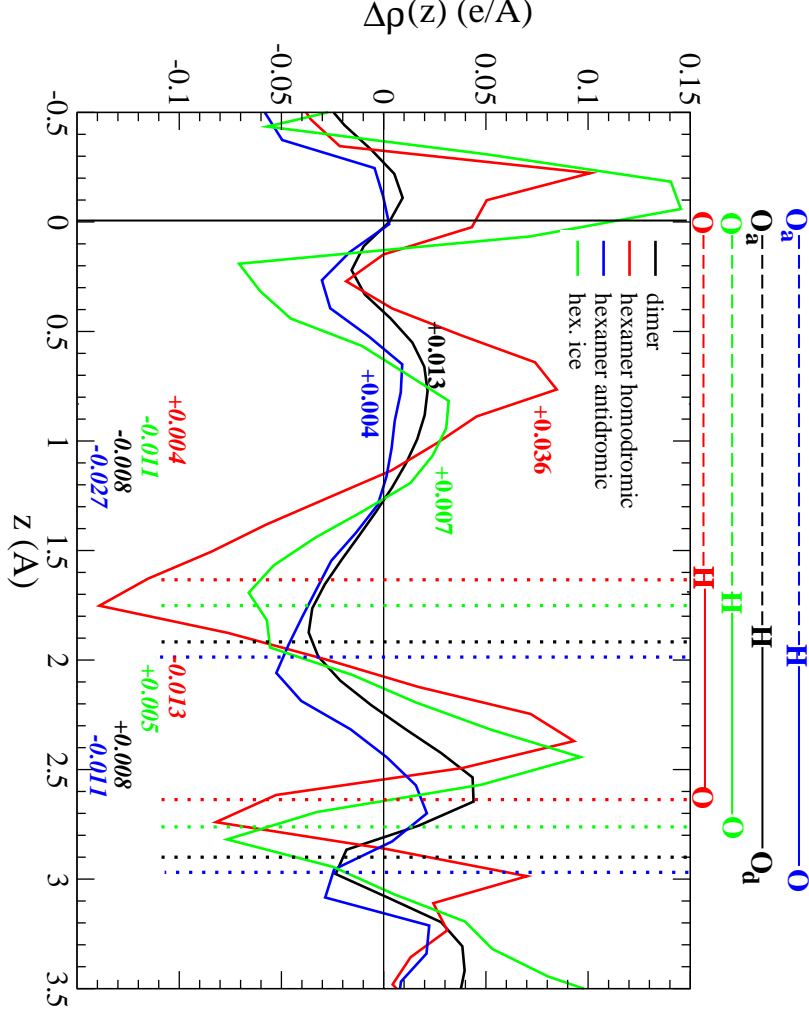


FIG. 8: Differential electron charge density, $\Delta\rho(z)$, for the water dimer, 2 cyclic water hexamers (*homodromic* and *antidromic* case), and hexagonal ice. Positive numerical values near the second peak indicate accumulation of the corresponding electron charge (in e) obtained by integral of $\Delta\rho(z)$ along z ; the numerical values in italics in the bottom indicate the electron charge (in e) between O and H (the HB region) and between H and O (the covalent bond region), respectively (these regions are delimited by vertical, dotted lines).

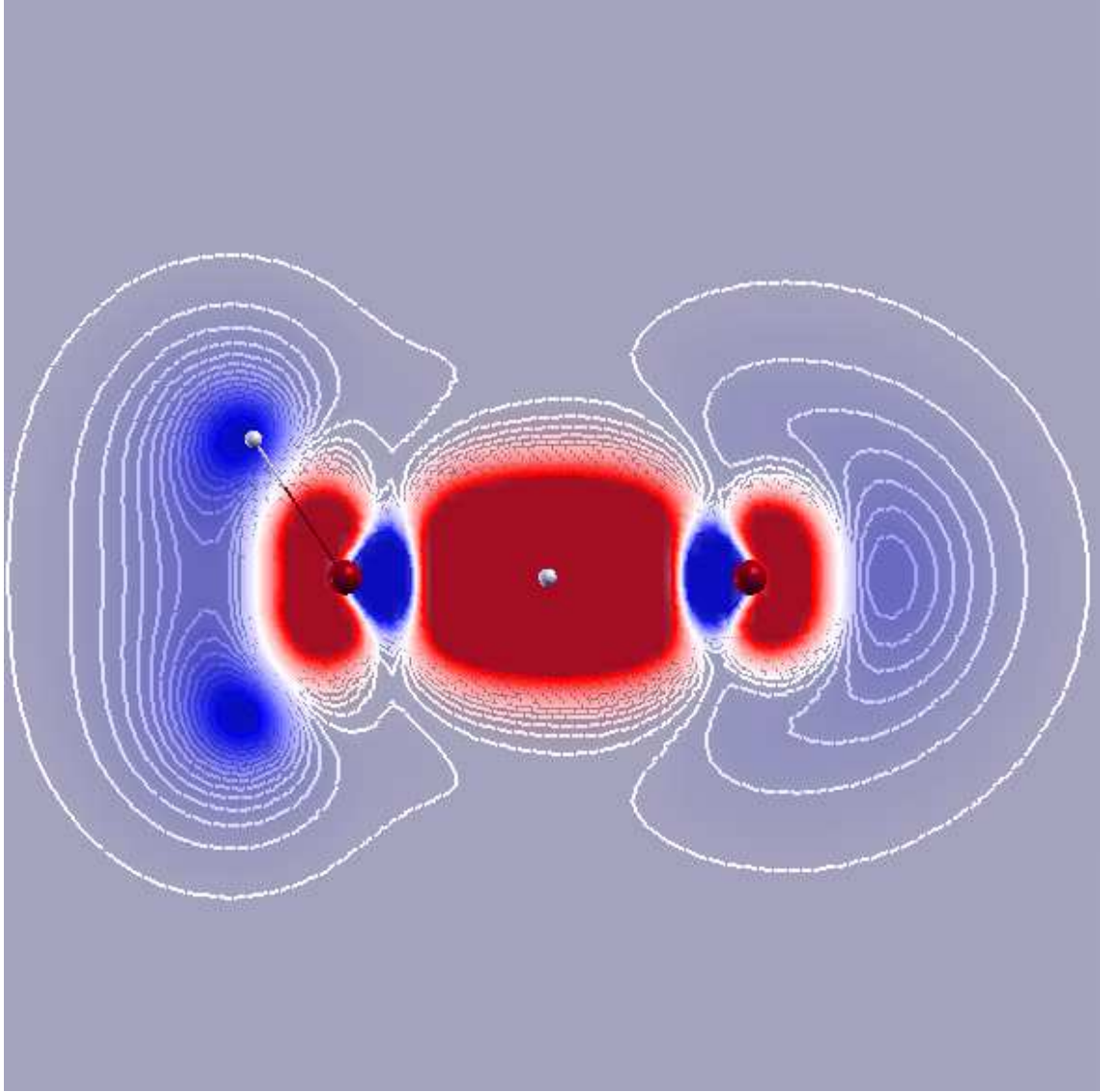


FIG. 9: Differential electron charge density, $\Delta\rho$, for the protonated water dimer in the $\text{H}_2\text{O}-\text{H}^+-\text{H}_2\text{O}$ (Zundel cation) configuration (shown is the difference between the dimer density and those of the isolated water molecules), plotted on a plane containing the two O atoms and H^+ . Red areas indicate electron density gain, while blue areas indicate loss of electron density; increments between contour lines correspond to $7 \times 10^{-4} e/\text{\AA}^3$ (within the range $\pm 0.01 e/\text{\AA}^3$).

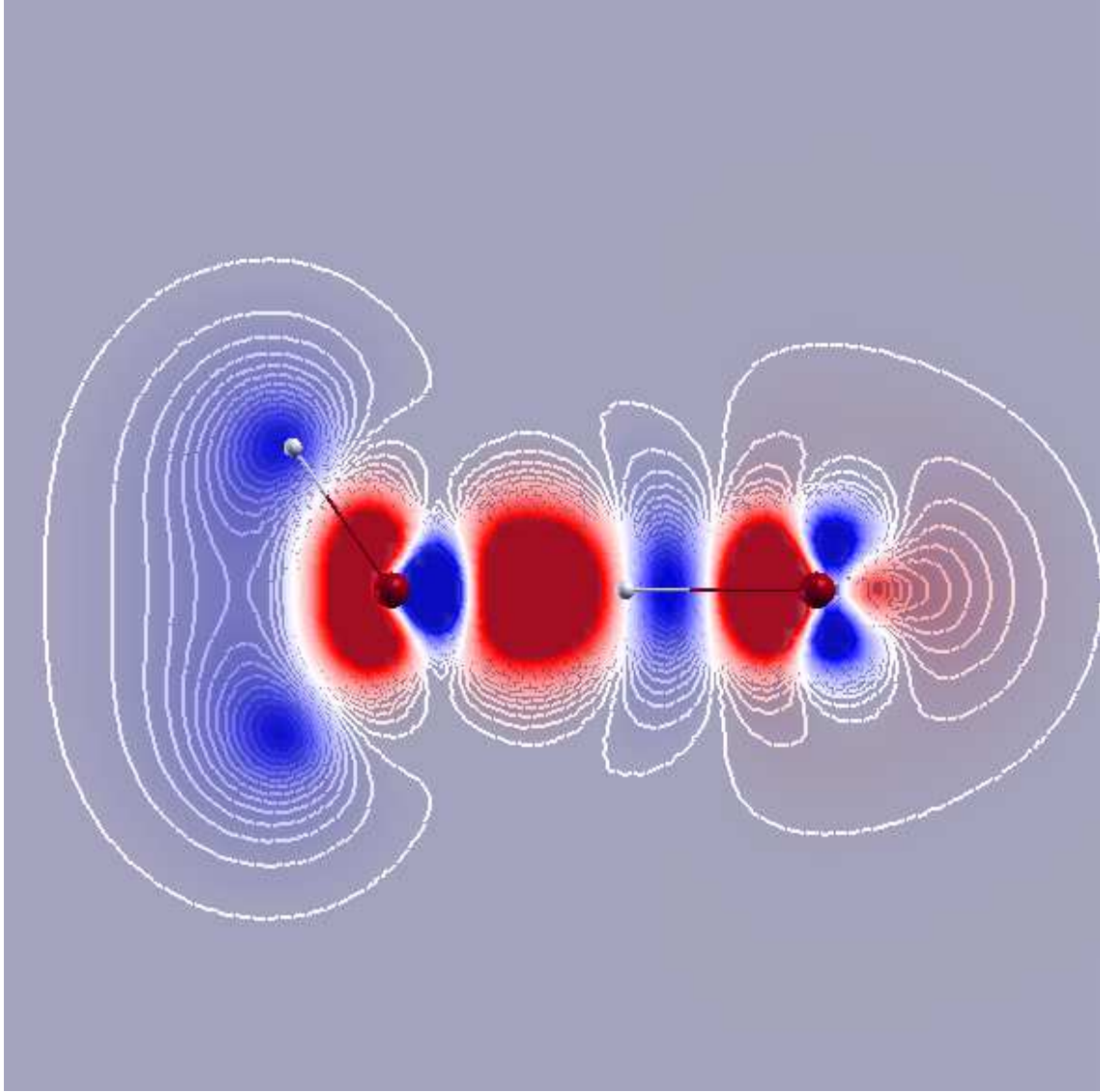


FIG. 10: Differential electron charge density, $\Delta\rho$, for the protonated water dimer in the $\text{H}_2\text{O}\cdots\text{H}^+-\text{H}_2\text{O}$ configuration (shown is the difference between the dimer density and those of the isolated water molecules), plotted on a plane containing the two O atoms and H^+ . Red areas indicate electron density gain, while blue areas indicate loss of electron density; increments between contour lines correspond to $7 \times 10^{-4} e/\text{\AA}^3$ (within the range $\pm 0.01 e/\text{\AA}^3$).

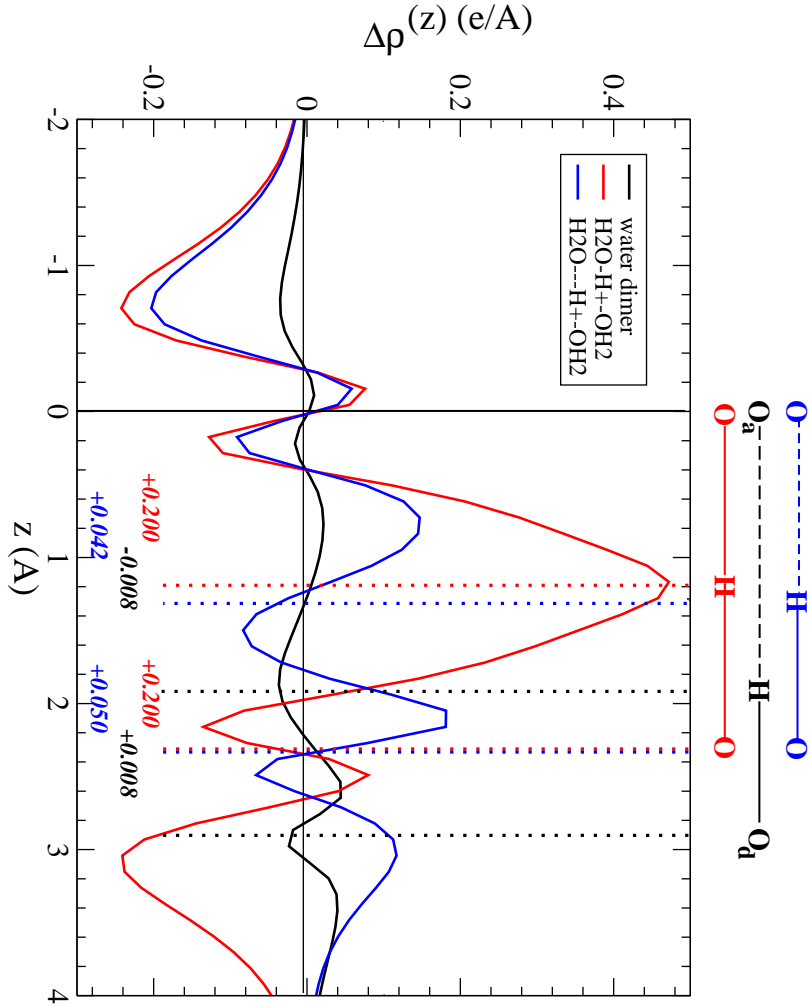


FIG. 11: Differential electron charge density, $\Delta\rho(z)$, for the water dimer and the protonated water dimer in two different configurations, $\text{H}_2\text{O}-\text{H}^+-\text{H}_2\text{O}$ (the Zundel cation) and $\text{H}_2\text{O}\cdots\text{H}^+-\text{H}_2\text{O}$. The numerical values in the bottom indicate the electron charge (in e) between O and H, and between H and O, that are the HB and the covalent bond region, respectively, for the water dimer and $\text{H}_2\text{O}\cdots\text{H}^+-\text{H}_2\text{O}$ (these regions are delimited by vertical, dotted lines).